Mine Water Environ (2011) 30:22–37
DOI 10.1007/s10230-010-0131-3

TECHNICAL ARTICLE

Kinetic Testing and Sorption Studies by Modified Weathering Cells to Characterize the Potential to Generate Contaminated Neutral Drainage

B. Plante · M. Benzaazoua · B. Bussière

Received: 12 April 2010 / Accepted: 3 December 2010 / Published online: 19 December 2010

Abstract Techniques developed for acid mine drainage (AMD) prediction might not be suitable for contaminated neutral drainage (CND) generating sites. The Tio mine waste is known to generate Ni contaminated neutral drainage in some of the piles, but humidity cell tests fail to generate the Ni concentrations observed in the field. Weathering cell tests (small-scale humidity cell tests) were performed on fresh and weathered (produced 25 years ago) waste rock samples from the Tio mine containing various levels of hemo-ilmenite ore, and results were compared to humidity cell results on similar samples. The main constituents of the waste rock are the hemo-ilmenite ore and the plagioclase gangue; these minerals were purified from the waste rocks and the purified fractions were also submitted to weathering cell tests. The fresh waste rock samples were also submitted to sorption cells (modified weathering cells), which showed that the waste rocks have an important Ni sorption potential and that the sorbed phases are stable under weathering cell conditions. Even though the Ni concentrations obtained from the laboratory tests remain significantly lower than those obtained in field conditions (from field test pads and from waste rock piles), the results from the present study give important insight into the geochemical processes implicated in CND generation.

Keywords Contaminated neutral drainage · Kinetic testing · Prediction · Sorption · Weathering cells

Introduction and Background

The oxidation of sulfide minerals within mine waste rocks and tailings, in the presence of sufficient neutralizing minerals, can lead to the formation of contaminated neutral drainage (CND). CND is characterized by metal concentrations greater than regulation criteria values at circum-neutral pH (Bussière 2007; MEND 2004; Nicholson 2004; Pettit et al. 1999). The present study was performed on waste rock samples from the Tio mine, a hematite-ilmenite (respectively, Fe_2O_3–$FeTiO_3$) deposit near Havre-Saint-Pierre, Québec, Canada, exploited since the early 1950s through an open pit operation by Rio Tinto, Iron and Titanium Inc. The gangue minerals of the Tio ore are mainly calcic plagioclases, which are close to labradorite composition (approximate formulae $Na_{0.4}Ca_{0.6}Al_{1.6}Si_{2.4}O_8$), and pyroxenes (Pepin 2009). The gangue also contains chlorite, mica, biotite, and sulfides as pyrite (FeS_2) and traces of millerite (NiS). Water draining from the waste rock piles is at near-neutral pH and sporadically

Electronic supplementary material The online version of this article (doi:10.1007/s10230-010-0131-3) contains supplementary material, which is available to authorized users.

B. Plante (✉) · M. Benzaazoua · B. Bussière
Univ du Québec en Abitibi-Témiscamingue (UQAT), 445, boul de l'Université, Rouyn-Noranda, QC J9X5E4, Canada
e-mail: benoit.plante@uqat.ca

B. Plante · M. Benzaazoua · B. Bussière
NSERC-Polytechnique-UQAT Chair, Environment and Mine Waste Mgmt, 445, boul de l'Université, Rouyn-Noranda, QC, Canada

M. Benzaazoua
Canada Research Chair on Integrated Mgmt of Mine Waste, UQAT, 445, boul de l'Université, Rouyn-Noranda, QC, Canada

B. Bussière
Canada Research Chair on the Restoration of Abandoned Mine Sites, UQAT, 445, boul de l'Université, Rouyn-Noranda, QC, Canada

shows Ni concentrations slightly higher than those allowed by applicable local regulations (Québec province, Canada).

Humidity cells tests and field experimental cells on fresh (<1 month since production) and weathered (approx. 25 years old) Tio mine waste rocks suggested that the waste rocks are not acid-generating in the long term (Pepin 2009; Plante et al. 2010a). The geochemical behaviours of the main minerals composing the Tio waste rocks (ilmenite, plagioclase, and pyroxenes) are well described in the literature and are summarized below.

For naturally weathered ilmenite, Grey and Reid (1975) first proposed a two-stage alteration mechanism that is currently the generally accepted model (Janßen et al. 2008; Mücke and Bhadra Chaudhuri 1991). In the first stage, ilmenite undergoes weathering through oxidation and removal of iron to form an apparently continuous series of compositions from ilmenite to pseudorutile (ideally, $Fe_2Ti_3O_9$) as a transitional phase, as depicted by Eqs. 1 (Lener 1997, after Mücke and Bhadra Chaudhuri 1991) or 2 (Lener 1997, after Grey and Reid 1975):

$$6Fe^{2+}TiO_3 + 3H_2O + 1.5O_2 \rightarrow 2Fe^{3+}Ti_3O_9 + 2Fe(OH)_3 \quad (1)$$

$$Fe^{2+}TiO_3 + 2H^+ + {}^1/_2O_2 \rightarrow Fe_2^{3+}Ti_3O_9 + Fe^{2+} + H_2O \quad (2)$$

Iron is assumed to diffuse out through the unaltered oxygen lattice. During this first alteration stage, iron is oxidized until all of the ilmenite Fe^{2+} is converted to Fe^{3+} within the pseudorutile. Ilmenite minerals may contain many substituents within its crystal structure, most notably Mg and Mn (e.g. Lener 1997, and references therein). Ilmenite dissolution is known to be associated with the release of Mg and Mn (e.g. Grey et al. 2005; Hodgkinson et al. 2008; Lener 1997; Nair et al. 2009; Schroeder et al. 2002). Once all of the Fe^{2+} is converted into Fe^{3+} and oxidation is completed, the second alteration stage starts, where pseudorutile hydrolyses and undergoes incongruent dissolution, resulting in the formation of rutile (TiO_2), anatase (TiO_2), and/or leucoxene (Frost et al. 1983; Mücke and Bhadra Chaudhuri 1991; Nair et al. 2009), which is believed to be the ultimate alteration product of ilmenite (Lener 1997; Nair et al. 2009; Schroeder et al. 2002). Rutile and leucoxene formation are described by Eqs. 3 and 4 (Lener 1997, after Mücke and Bhadra Chaudhuri 1991) or Eq. 5 (Grey and Reid 1975):

$$Fe_2^{3+}Ti_3O_9 + 3H_2O \rightarrow Fe^{3+}Ti_3O_6(OH)_3 + Fe(OH)_3 \quad (3)$$

$$Fe^{3+}Ti_3O_6(OH)_3 \rightarrow 3TiO_2 + Fe(OH)_3 \quad (4)$$

$$Fe_2^{3+}Ti_3O_9 \rightarrow 3TiO_2 + Fe_2O_3 \quad (5)$$

Plagioclases are a solid solution series belonging to the feldspar family. The series range from albite to anorthite end members with respective compositions of $NaAlSi_3O_8$ and $CaAl_2Si_2O_8$, where Na and Ca atoms can substitute for each other in the mineral's crystal lattice structure. Plagioclase dissolution has long been known to be incongruent, with Al, Na, and Ca being preferably dissolved at the surface (Blum and Stillings 1995; Carroll and Knauss 2005; Casey et al. 1989; Inskeep et al. 1991; Muir et al. 1989, 1990a, b; Schweda et al. 1997). This dissolution generates an Al-Na-Ca-poor thin layer at the plagioclase surface (Blum and Stillings 1995). The formation of silica-enriched residual layers on feldspars in acidic solution is a multi-step process, in which Ca and Na are incongruently released from the surface, followed by Al, and finally by Si in a later weathering stage (Blum and Stillings 1995; Muir and Nesbitt 1997; Muir et al. 1990b; Schweda et al. 1997).

According to Blake and Walter (1999), the thickness and composition of the leached layers on feldspars depends on solution composition and pH. Dilute acidic conditions produce relatively thick Si-rich layers, up to several thousand angstroms (Blum and Stillings 1995; Casey et al. 1989; Muir and Nesbitt, 1992; Hellmann 1995; Muir and Nesbitt 1997; Nesbitt and Skinner 2001), whereas dissolution at near-neutral pH (between 5 and 8) produces only thin weathered layers that are tens of angstroms thick (Blake and Walter 1999; Blum and Stillings 1995; Muir and Nesbitt 1997). The circumneutral environments prevailing in the Tio mine waste rock kinetic tests would be expected to promote the formation of such thin weathered layers on the plagioclase feldspar surfaces.

The Al released from labradorite dissolution could precipitate as various possible secondary phases, such as hydroxide $Al(OH)_3$ or kaolinite ($Al_2Si_2O_5(OH)_4$). The labradorite reaction under acidic conditions leading to kaolinite precipitation can be generalized and simplified as Eq. 6, while the same reaction leading to aluminum hydroxide is generalized as Eq. 7:

$$Ca_{0.6}Na_{0.4}Al_{1.6}Si_{2.4}O_8 + 1.6H^+ + 2.4H_2O \rightarrow 0.8Al_2Si_2O_5(OH)_4 + 0.8H_4SiO_{4(aq)} + 0.4Na^+_{(aq)} + 0.6Ca^{2+}_{(aq)} \quad (6)$$

$$Ca_{0.6}Na_{0.4}Al_{1.6}Si_{2.4}O_8 + 1.6H^+ + 6.4H_2O \rightarrow 1.6Al(OH)_3 + 2.4H_4SiO_{4(aq)} + 0.4Na^+_{(aq)} + 0.6Ca^{2+}_{(aq)} \quad (7)$$

The pyroxenes found in the Tio mine waste rocks are represented mainly by enstatite (Plante et al. 2010b), which can neutralize acid through Eq. 8 (Oelkers and Schott 2001; Stefánsson 2001):

$$MgSiO_3 + 2H^+ + H_2O \rightarrow Mg^{2+} + H_4SiO_4 \quad (8)$$

Pyroxenes incongruently release Mg over Si in early dissolution stages, much like the plagioclases preferentially

release Ca and Na over Si initially. The preferential release of Mg from pyroxene is expected to lead to the formation of a Mg-depleted and Si- and H-enriched surfaces (Oelkers et al. 2009; Zakaznova-Herzog et al. 2008).

Most Ca, Al, and Si releases from the Tio waste rocks are due to plagioclase and pyroxene weathering, in response to the oxidation of pyrite, which produces S (as sulfates) and acidity. Mg release is related to ilmenite and pyroxene dissolution, while Mn release is mainly associated with ilmenite.

Batch sorption studies conducted on Tio mine waste rocks and on purified mineral fractions of those waste rocks have clearly demonstrated that ilmenite and plagioclase exhibit significant Ni-sorption properties (Plante et al. 2008, 2010b). Sequential chemical extractions also suggest that the sorbed Ni is stable under oxidizing conditions but can be released under reducing conditions. These studies provided important insight into the Tio mine waste rock geochemical behavior, but were conducted in conditions different from those of the humidity cells (closed vs. open leaching systems). The extent of applicability of the results to kinetic testing was thus questionable, particularly the importance of sorption phenomena and the stability of the sorbed Ni phases in kinetic testing conditions. Nevertheless, humidity cell studies did not generate Ni concentrations in the leachates close to those encountered in field studies (Pepin 2009; Pepin et al. 2008), which are more representative of the Ni concentrations in CND released from some of the actual waste rock piles at the mine site.

To better understand the geochemical behavior of the Tio mine waste rock under laboratory kinetic testing conditions, we decided to conduct a geochemical study of the main minerals composing the Tio mine waste rock using weathering cells, which are small-scale humidity cells requiring less than 100 g and proven to provide similar results to humidity cells (Villeneuve et al. 2004). In order to validate that the response of the two types of tests were similar for the Tio mine waste rocks, weathering cell tests were performed on the same Tio mine waste rocks that were studied in the humidity cells (Plante et al. 2010a). Weathering cells were also performed on purified mineral fractions of ilmenite and plagioclase prepared from the Tio mine waste rock (Plante et al. 2010b). In addition to the weathering cells, kinetic sorption studies were performed on the same fresh waste rock samples. Results from this study will enable a more precise understanding of the geochemical processes driving CND formation in waste rock piles at the Tio mine by providing more insight to sorption processes in kinetic testing conditions, the relative stability of the sorbed phases, and the geochemical behaviour of the main minerals composing the waste rock.

Materials and Methods

Samples Choice and Preparation

Since the Tio mine has been in operation since 1950, waste rock there has been submitted to natural weathering phenomena over time periods ranging from a few days to several decades. Moreover, the waste rock piles composition varies significantly, as the target cut-off for milling is approximately 76% hemo-ilmenite. Waste rock samples were carefully selected to cover a wide spectrum of hemo-ilmenite content for both freshly produced waste rocks (C1–C3) and waste rocks that had weathered for 25 years (C4–C6). Table 1 lists the general characteristics of the samples selected for the present study, the ilmenite levels targeted during sampling, and the approximate age of the samples. The fresh waste rock samples (C1–C3) had hemo-ilmenite content of C1 < C2 < C3, while the weathered waste rock (C4–C6) had hemo-ilmenite contents of C4 < C5 <C6. All samples were screened to < 10 cm at the mine site and to <500 μm for use in the present study; it is recognised that the finer fractions are responsible for most of the geochemical behaviour of waste rocks (e.g. Price and Kwong 1997). Grinding was avoided in order to preserve the surface states of the weathered waste rock

Table 1 Physical characteristics of the waste rock samples studied (D_x, in μm, refers to the size for which x% of the sample is under this grain size; S.S.A. in m^2/g)

	Ilmenite level	Approx. age	G_s	S.S.A.	% <80 μm	D_{10}	D_{50}	D_{90}
Ilmenite	>95%	Unknown	4.79	0.093	3	91	164	265
Plagioclase	Traces	Unknown	2.69	0.080	3	99	187	275
C1	Low	1 month	3.09	0.837	21	18.3	279	603
C2	Intermediate		3.42	0.863	32	7.57	194	542
C3	High		3.76	0.778	16	34.7	361	651
C4	Low	25 years	3.27	1.93	24	14.7	254	585
C5	Intermediate		3.50	1.79	23	14.2	270.4	584.5
C6	High		3.60	1.52	23	14.0	292.9	626.7

samples. Purified mineral fractions were prepared at CO-REM from the Tio mine waste rocks. Many concentration methods were combined (magnetic and gravimetric separations, flotation) to obtain relatively pure fractions of the main minerals of the Tio mine waste rocks: ilmenite, plagioclase, sulfides, mica, chlorite, and spinel. All fractions were sieved at +200-48 mesh (75–300 μm). Only the hemo-ilmenite and plagioclase samples are considered in this paper because they are the most important sorbing minerals (see Plante et al. 2010b).

Characterization Methods

The specific gravity (G_s) of the waste rock samples was determined with a Micromeritics helium pycnometer. The specific surface area (S.S.A.) was determined using a Micromeritics surface area analyser using the B.E.T. method (Brunauer et al. 1938). The grain size distribution (Merkus 2009) was obtained by sieving for the fractions between 10 cm and 0.355 μm, and by a laser diffraction grain size analyzer for the <0.355 μm fraction (using a Malvern Instruments Mastersizer S). The Tio mine waste rock chemical analysis was performed using an acid digestion (HNO_3-Br_2-HF-HCl) followed by ICP-AES analysis for over 20 elements, to a 0.001 wt% precision. Silicon is partially evaporated during the digestion procedure and therefore is not reported for this study. Sulfide sulfur was determined by subtraction of the sulfate sulfur (determined by a 40% HCl extraction with 0.001 wt% precision; Sobek et al. 1978) from the total sulfur (ICP-AES analysis). The pH values of the leachates were measured with an Orion triode electrode (temperature compensated) with an Orion 920A controller, while the electrical conductivity was measured with an OAKTON Acorn Series CON 6 electrical conductivity meter. Aliquots of the leachates were acidified to 2% HNO_3 for conservation until analysis by ICP-AES. The mineralogical characterization was performed with a Bruker A.X.S. D8 Advance X-ray diffraction (XRD) instrument, with a detection limit and precision of approximately 0.1–0.5 wt%. Mineralogical quantification was realized with Rietveld (1993) fitting of the XRD data using TOPAS software. Acid–base accounting (ABA) was determined using the protocol described by Lawrence and Wang (1997). The acid-generation potential (AP) was calculated assuming that the sulfide sulfur content was exclusively expressed as pyrite and that all pyrite was available for oxidation, and converted to calcite equivalents (kg $CaCO_3$/t), with a precision of 5–7%. The neutralization potential (NP) was determined by HCl additions and back-titration of the excess acid to a pH 8.3 endpoint, with a precision of ±2 kg $CaCO_3$/t. The net neutralization potential (NNP) is the difference between the AP and NP (NNP=NP-AP), and the NP/AP ratio was also determined.

A Hitachi S-3500N scanning electron microscope (SEM) was used for further mineralogical characterizations on the samples. Backscattered electrons imaging mode (BSE) was employed for polished section observations (waste rocks impregnated in epoxy resin), while secondary electrons imaging mode (SE) was employed for the observation of free particles deposited on a carbon adhesive. Chemical analyses on the SEM were performed with energy dispersive spectrometry (EDS) of an Oxford Instruments 20 mm^2 X-Max silicon drift detector (SDD) X-ray probe under the INCA system, with oxygen determined stoichiometrically.

Weathering Cells

The geochemical behaviours of the pure ilmenite, plagioclase and Tio mine waste rock samples were evaluated using small scale leaching cells called weathering cells (Cruz et al. 2001; Villeneuve et al. 2004). The weathering cells consist of bi-weekly flushes (typically Mondays and Thursdays) by deionized water (50 mL) on 40–70 g of a sieved fraction (< 500 μm) of the samples; grinding was avoided for surface preservation considerations (Plante et al. 2010a). The samples were allowed to dry under ambient air between flushes. Figure 1a shows the schematic illustration of a weathering cell.

Kinetic Sorption Studies (Sorption Cells)

Kinetic sorption studies were performed using modified weathering cells (called sorption cells), in which the leaching water was not deionized water, but instead was

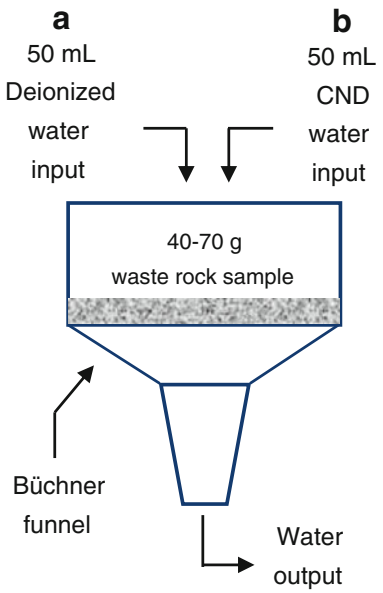

Fig. 1 Schematic illustration of the weathering (a) and sorption (b) cells used in this study

actual CND from the mine site. The comparison of metal concentrations in the leachates with those of the contaminated leaching water enables the determination of the sorbed quantities in the sorption cells. Thus, sorption cells were run on fresh waste rock samples in addition to classic weathering cells; weathered waste rocks were not submitted to kinetic sorption studies because their sorption capacities were proven to be much less significant than those of the fresh ones in batch sorption studies (Plante et al. 2010b). Figure 1b shows the schematic illustration of a sorption cell. The contaminated water sampled at the mine site contained 2.26 mg/L Ni, 0.63 mg/L Co, 276 mg/L S, 285 mg/L Ca, 70.6 mg/L Mg, 0.42 mg/L Mn, 6.74 mg/L Si, and 0.19 mg/L Zn, at a pH of 7.8 and an electrical conductivity of 2228 µS/cm.

Results and Discussion

Physical, Chemical and Mineralogical Properties

The physical characteristics of the samples studied are summarized in Table 1. The G_s of the hemo-ilmenite samples ranged from 4.74 to 4.79, consistent with pure ilmenite (4.70–4.79) G_s values. The G_s of the plagioclase sample was 2.69, in accordance with the pure labradorite G_s value (Klein et al. 1977). The G_s of the waste rock samples varied between 3.09 and 3.76 and was correlated to the hemo-ilmenite levels targeted during sampling. The S.S.A. of the pure minerals samples varied between 0.08 and 0.10 m^2/g whereas those of the waste rock samples varied between 0.78 and 1.93 m^2/g; the differences are attributed to the variations in terms of grain size distributions (pure minerals: 75–300 µm; waste rocks: <500 µm). The D_{10}, D_{50} and D_{90} values respectively represent the grain size for 10, 50, and 90% passing on the cumulative grain size distribution curve. The purified fractions had 3% <80 µm, whereas the waste rock samples had 16–32% <80 µm, and also significant differences in D_{10} (purified fractions: 91–99 µm, waste rocks: 7–35 µm), D_{50} (purified fractions: 164–187 µm, waste rocks: 194–361 µm) and D_{90} (purified fractions: 265–275 µm, waste rocks: 542–651 µm) values. The fact that the S.S.A. of the fresh (C1–C3) waste rock samples (0.78–0.86 m^2/g) were about half of those of the weathered (C4–C6) ones (1.5–1.9 m^2/g) could be due to the greater surface roughness and/or the precipitation of secondary minerals associated with weathering.

The chemical and mineralogical characteristics of the samples are summarized in Tables 2 and 3, respectively. Most heavy metals (Co, Cr, Mn, Ni) as well as Mg are associated with ilmenite (and its sulfide content) rather than with plagioclase, as demonstrated by Plante et al. (2010b). Ca and Al levels show that residual plagioclase was present in the ilmenite samples, whereas Ti and Fe levels show that small amounts of hemo-ilmenite were present in the

Table 2 Chemical and ABA characterization of the samples studied (elements in wt%; AP, NP, and NNP in kg $CaCO_3$)

	Ilmenite	Plagioclase	C1	C2	C3	C4	C5	C6
Al	0.341	13.0	9.26	6.86	4.65	6.46	5.30	4.74
Ba	<ldm	0.026	0.022	0.017	0.013	0.019	0.016	0.014
Ca	0.060	6.56	4.50	3.27	2.30	3.09	2.37	2.11
Co	0.049	0.000	0.020	0.031	0.042	0.024	0.033	0.034
Cr	0.085	0.001	0.020	0.032	0.054	0.046	0.055	0.063
Cu	0.006	0.002	0.023	0.041	0.046	0.025	0.032	0.032
Fe	42.3	0.431	12.8	20.6	30.7	17.5	26.3	29.3
Mg	1.56	0.196	0.954	1.51	1.71	3.06	2.58	2.56
Mn	0.107	0.002	0.035	0.054	0.074	0.073	0.075	0.079
Ni	0.031	0.002	0.022	0.049	0.044	0.031	0.032	0.038
S_{total}	0.186	0.032	0.543	0.533	0.755	0.215	0.350	0.382
$S_{sulphate}$	<ldm	<ldm	0.035	0.052	0.027	0.022	0.021	0.020
$S_{sulphide}$	0.186	0.032	0.508	0.481	0.728	0.193	0.329	0.362
Sb	0.064	0.001	0.007	0.013	0.019	0.010	0.014	0.024
Ti	20.1	0.057	5.99	10.8	14.7	7.70	11.1	12.2
Zn	0.005	0.004	0.004	0.005	0.005	0.007	0.006	0.006
AP	5.8	1.0	15.9	15.0	22.8	6.0	10.3	11.3
NP	3.7	4.3	11.1	12.3	14.6	10.5	8.0	6.4
NNP	−2.1	3.3	−4.7	−2.7	−8.1	4.5	−2.3	−4.9
NP/AP	0.64	4.3	0.70	0.82	0.64	1.74	0.78	0.56

Table 3 XRD mineralogical characterization of the samples studied (in wt%)

Mineral	Formulae	Ilmenite	Plagioclase	C1	C2	C3	C4	C5	C6
Labradorite	$(Ca,Na)(Si,Al)_4O_8$		98.5	N/A	42.8	27.5	38.7	31.1	31.7
Ilménite	$FeTiO_3$	73.3			21.1	26.0	18.9	25.0	26.6
Hématite	Fe_2O_3	26.7			6.4	7.1	7.0	8.7	9.2
Pyrite	FeS_2				1.6	2.3	0.9	1.4	1.8
Chalcopyrite	$CuFeS_2$				0.6	0.6	0.1	0.3	0.3
Enstatite	$Mg_2Si_2O_6$				15.5	20.6	24.9	23.7	20.5
Pigeonite	$(Mg,Fe^{2+},Ca)(Mg,Fe^{2+})Si_2O_6$				1.7	3.0	1.8	1.9	2.1
Biotite	$K(Mg,Fe^{2+})_3(Al,Fe^{3+})Si_3O_{10}(OH,F)_2$				2.1	1.3	0.9	1.1	1.1
Muscovite	$KAl_2\ (Si_3Al)O_{10}(OH,F)_2$				2.6	3.1	1.7	1.4	0.6
Chlorite	$(Mg,Fe,Al)_6(Si,Al)_4O_{10}(OH)_8$		1.5		0.8	0.3	1.2	0.9	0.7
Orthoclase	$KAlSi_3O_8$				1.3	1.2	1.9	1.5	2.7
Rutile (anatase)	TiO_2				1.8	2.0	1.2	1.9	1.6
Spinel	$MgAl_2O_4$				0.4	3.5	0.4	0.4	0.6
	Total	100.0	100.0		98.8	98.5	99.5	99.2	99.3

plagioclase sample. Sulfide levels were higher in the fresh (0.48–0.73 wt%) waste rock than in the weathered samples (0.19–0.36 wt%). Ca (2.1–4.5 wt%) and Al (4.6–9.3 wt%) levels followed the inverse of Fe (13–31 wt%) and Ti (6–15 wt%) in the waste rock samples. The AP and NP values were all fairly low (AP<16 kg $CaCO_3$/t; NP<15 kg $CaCO_3$/t), leading to NNP values within the uncertainty zone and NP/AP ratios around 1 (except for plagioclase, with over 4). Considering the low NP values and the absolute uncertainty of the method (±2 kg $CaCO_3$/t, based on a 39 kg $CaCO_3$/t reference sample; Plante 2005), the relative errors ranged from 13 to 33%. As a result, ABA interpretation from such low values is difficult. Minerals other than ilmenite and hematite in the hemo-ilmenite samples were undetectable by XRD, while some chlorite was detectable in the plagioclase sample, dominated by labradorite (see Table 3). Other minerals present included pyroxenes (enstatite and pigeonite), muscovite, chlorite, biotite, orthoclase, rutile, sulfides, orthoclase, and spinel.

Weathering Cells on Waste Rock Samples

Some of the geochemical results of the waste rock samples submitted to weathering cells are presented in Figs. 2 and 3. The pH values of the leachates remained near-neutral throughout the tests, with the pH values of the weathered samples (7.0–7.5) being slightly lower than those of the fresh waste rock (7.5–8.0). The conductivity values were lower in the weathered waste rocks (10–20 µS/cm) than in the fresh ones (50–100 µS/cm). The Ca and Al concentrations were higher in the leachates from the fresh waste rocks (Ca: around 10 mg/L; Al: up to 0.30 mg/L) than those of the weathered ones (Ca: around 1 mg/L; Al: around 0.02 mg/L), whereas the Si and Mg concentrations generated by the weathered waste rocks are greater (Si: 10–100 mg/L; Mg: 0.5–0.8 mg/L) than those of the fresh ones (Si: 5–20 mg/L; Mg: around 0.1 mg/L). All waste rock samples generated similar S concentrations (all S was assumed to be present as sulfates in the present study) in the leachates (0.1–1.0 mg/L), while Ni levels tended to increase throughout the test (up to 0.026 mg/L), although the weathered waste rocks generated detectable Ni concentrations more often than the fresh ones (detection limit of 0.004 mg/L). Mn concentrations increased throughout the tests (up to 0.020 mg/L), and weathered waste rocks generated detectable levels (detection limit: 0.002 mg/L) more frequently than fresh ones, with the exception of the C2 sample, for which Mn generation was significantly greater than other samples from 175 days on (0.01–0.02 mg/L). These weathering cell results are similar to those previously obtained using humidity cells (Plante et al. 2010a).

The mass of each metal found in the leachates were added up and normalized to the total sample mass (mg/kg). The slope of the linear regression within the stabilized portion of these cumulative normalized loadings over time gives the elemental release rates (mg/kg/day); the most relevant for the present study are shown in Table 4. It is important to point out the difference between the weathering rate and the release rate. According to Sapsford et al. (2009), the weathering rate is defined as the rate (mass per unit time, often normalized to unit mass or unit area) at which a primary mineral is transformed into secondary products, whether soluble or insoluble, congruently or incongruently, whereas the release rate is the rate at which an element or species is driven away from a unit mass of

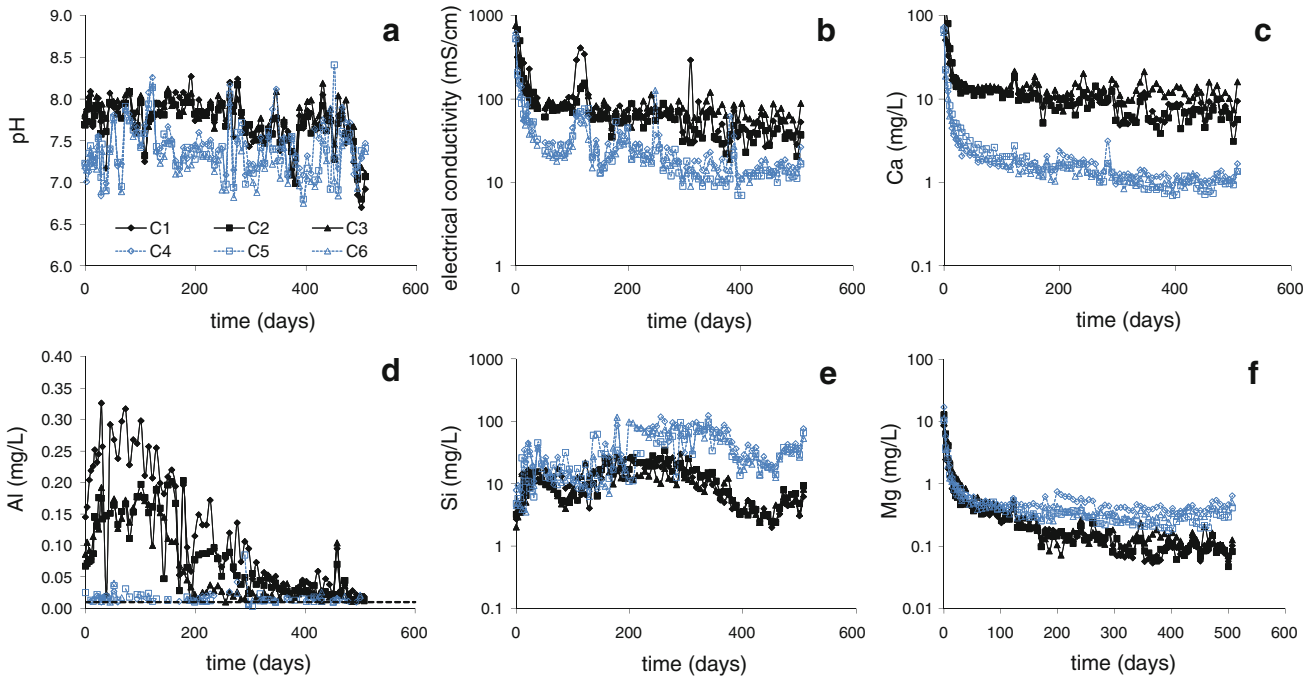

Fig. 2 Weathering cell results for waste rocks samples (note: log scale for all but pH and Al)

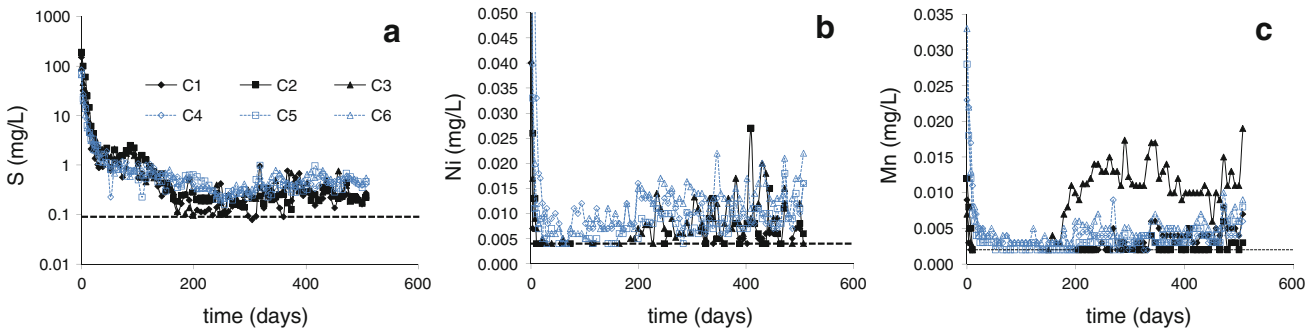

Fig. 3 Weathering cell results on waste rock samples

rock per unit time. In kinetic tests such as those used in the present study, the release rate is stoichiometrically related to the weathering rate of a given primary mineral only when the considered reaction products are entirely flushed from the material. The cumulative normalized loadings of some elements from the waste rocks weathering cells are presented as Electronic Supplementary Material (ESM), while the release rates are presented in Table 4. The cumulative Ca levels of the fresh waste rocks were significantly greater than those of the weathered ones; the Ca release rates corresponding to fresh waste rocks (1.4–2.4 mg/kg/day) were almost an order of magnitude greater than for weathered samples (0.20–0.28 mg/kg/day). The cumulative Al levels corresponding to the fresh waste rocks were also significantly greater than the weathered ones during the first 100 days, but Al generation decreased to levels similar to the weathered waste rocks after 200 days. The Si generation was significantly greater in the case of weathered waste rocks, with three distinct phases with different release rates (slower until 200 days, faster from 200 to 350 days, then slower for the balance of the test); the release rates in Table 4 were calculated from the >350 days phase. Mg generation was slightly higher for weathered waste rocks (0.05–0.08 mg/kg/day) that for fresh ones (0.02–0.03 mg/kg/day). The S generation of all waste rocks was similar, with S release rates corresponding to weathered waste rocks being slightly higher (0.068–0.080 mg/kg/day) than fresh ones (0.039–0.055 mg/kg/day).

These results are similar to the humidity cell results (Plante 2010; Plante et al. 2010a). Although the dissolution of neutralizing minerals is exaggerated in weathering cells compared to humidity cells (Plante 2010), the general observations are the same: Ca and Al generation in

Table 4 Release rates (mg/kg/d) of selected elements in weathering cells (>150 days for all but post-sorption samples, >400 days) and associated determination coefficients (R^2), in parentheses

	Ca	Mg	Mn	Ni	S	Si	S/Ni	Ca/Si	Mg/Mn	Ni/Mn
Ilm	0.15 (0.95)	1.2E-02 (0.98)	1.1E-03 (0.98)	1.4E-02 (0.97)	4.1E-02 (0.98)	0.45 (0.92)	2.9	0.34	11	12
Plagio	0.69 (0.99)	1.9E-02 (0.99)	1.0E-03 (0.99)	1.0E-04 (0.55)	1.4E-02 (0.96)	0.48 (1.0)	137	1.5	19	0.10
C1	1.5 (1.0)	1.9E-02 (0.99)	5.8E-04 (0.95)	2.7E-04 (0.64)	4.4E-02 (0.98)	2.1 (0.91)	165	0.71	32	0.46
C2	1.4 (0.99)	2.0E-02 (0.98)	3.4E-04 (0.96)	6.6E-04 (0.87)	3.9E-02 (0.99)	2.5 (0.91)	59	0.55	60	2.0
C3	2.4 (1.0)	2.6E-02 (1.0)	2.2E-03 (1.0)	1.6E-03 (0.99)	5.5E-02 (0.97)	1.8 (0.95)	35	1.3	12	0.72
C4	0.28 (0.97)	7.7E-02 (0.99)	5.9E-04 (0.99)	1.7E-03 (1.0)	6.8E-02 (0.99)	10 (0.98)	40	2.7E-02	129	2.9
C5	0.21 (0.98)	4.9E-02 (0.99)	6.5E-04 (0.99)	1.5E-03 (0.99)	7.5E-02 (0.99)	8.1 (0.98)	49	2.5E-02	76	2.4
C6	0.20 (0.99)	5.7E-02 (1.0)	9.0E-04 (1.0)	2.5E-03 (1.0)	8.0E-02 (0.99)	9.1 (0.96)	32	2.2E-02	64	2.8
C1-GR (post-sorp)	3.0 (1.0)	0.14 (0.99)	2.5E-03 (1.0)	2.1E-03 (0.96)	0.67 (0.98)	0.49 (0.96)	315	6.1	55	0.85
C2-GR (post-sorp)	2.8 (1.0)	0.17 (0.99)	1.7E-03 (1.0)	2.0E-03 (0.96)	0.74 (0.97)	0.79 (0.95)	363	3.6	102	1.2
C3-GR (post-sorp)	3.0 (1.0)	0.10 (0.98)	3.3E-03 (1.0)	3.4E-03 (0.95)	0.47 (0.95)	0.57 (0.98)	135	5.3	31	1.0

drainage waters are greater in fresh waste rocks, while Si and Mg generation are greater in weathered waste rocks, and S generation is similar. Such similarities justify the use of weathering cells to study the geochemical behaviour of the purified mineral fractions by weathering cells, and the use of sorption cells to study sorption phenomena within waste rocks.

Weathering Cells on Ilmenite and Plagioclase

The geochemical behaviours of ilmenite and plagioclase samples from the Tio mine waste rocks were also investigated in weathering cells. Particularly, it was hoped that these tests would help determine whether the Ni in drainage waters is generated from sulfides or from Ni traces within the ilmenite and plagioclase minerals.

The weathering cell results of the hemo-ilmenite and plagioclase samples are shown in Fig. 4. The pH remains near-neutral throughout the tests (between 6.5 and 8.0). The Ca and Si were released by the plagioclase, which was also present as a minor impurity in the ilmenite sample. The Ca concentrations decreased throughout the test (from 10 to less than 0.5 mg/L) in the ilmenite samples; Ca was depleted by over 30% at the end of the test (Plante 2010). Along with the decrease in Ca concentrations, these results suggest that the available plagioclase surfaces were significantly depleted. The S concentrations (representing sulfate production) show that the sulfide traces oxidize in the hemo-ilmenite sample, whereas very few leachates contained detectable S concentrations form the plagioclase sample. Therefore, it appears that the sulfides in the plagioclase sample oxidize at rates too slow to produce detectable S concentrations in most of the leachates.

The Ni and Co concentrations generated by the hemo-ilmenite sample increased until approximately 450 days (up to 0.16 mg/L for Ni and up to 0.023 mg/L for Co), after which they decreased. There is a lag time before Ni and Co increases, probably due to the sorption properties of the hemo-ilmenite: the Ni and Co concentrations increased more rapidly after approximately 200–250 days. The decrease in Ni and Co concentrations observed after 450 days corresponds to a decrease in S concentrations from 450 days on, suggesting that the depletion of the sulfides available for oxidation was slowing the S production down to levels close to the detection limit (0.09 mg/L). However, the depletions are fairly low for S, Ni, and Co in the hemo-ilmenite sample (more than 98 % remaining at the end of the test; see Plante 2010). The low depletion levels of Ni and Co in the ilmenite sample are explained by sorption, which removed a significant part of the leached Ni and Co (and therefore not considered in the depletions), as demonstrated elsewhere (Plante et al. 2010b). The low Ni and Co concentrations in the leachates are explained at least in part by the low sulfide content of the hemo-ilmenite sample (0.186% $S_{sulfide}$), by complete oxidation of the ultrafine particles and passivation of the sulfide surfaces available for oxidation (Pepin 2009; Plante et al. 2010a). In addition, the Ni and Co in the hemo-ilmenite sample are not only attributable to sulfides, but were also present at trace levels within the ilmenite crystal lattice (Plante 2010; Plante et al. 2010b). The plagioclase sample does not produce detectable levels of Ni or Co in weathering cells because of the trace sulfide content (0.032 wt% $S_{sulfide}$) and because of the sorption properties of the sample.

Some of the cumulative normalized loadings from the pure minerals samples are shown in ESM 2 and 3. The

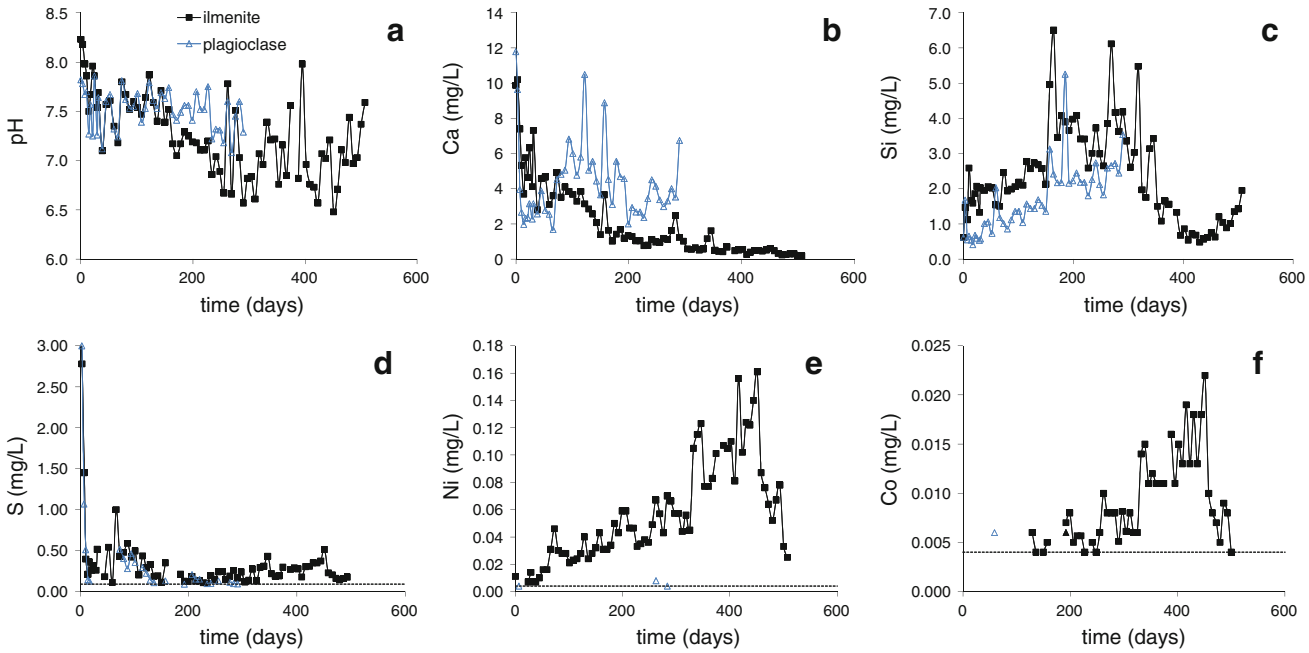

Fig. 4 Weathering cell results for pure minerals samples

release rates of Ca, Al, and Si loadings stabilized after 100 days for Ca and Al and after 300 days for Si (ESM 2a, 2b, and 2c, respectively). These results suggest that the plagioclase within the hemo-ilmenite sample almost ceased to react after 300 days; the Ca and Al generation significantly decreased after 100 days, while the Si generation did so after 300 days. This reactivity sequence is in accordance with the known labradorite reactivity mentioned in the introduction of this paper: Ca and Al were preferentially released in an early dissolution stage, and Si release peaked as weathering progressed further. In contrast, the Ca release from labradorite in the plagioclase sample did not decrease during the test (ESM 2a), suggesting that its dissolution remained at an early stage. Moreover, the total Ca generated by the plagioclase sample was close to that of ilmenite, despite the fact that the ilmenite sample only contained labradorite at trace levels.

In the first 100 days, the Ca production of the ilmenite and plagioclase samples was similar, but the Ca production in the ilmenite samples decreased afterwards (ESM 2a). The Ca release rate after 200 days (Table 4) from the plagioclase sample was 3–5 times greater than from the ilmenite samples. Also, the Si production in ilmenite samples slowed down after 300 days (ESM 2c), suggesting that the reactivity of the trace plagioclase levels in the ilmenite samples decreased. In comparison, the total Si generation in the plagioclase sample was small compared to that of the ilmenite sample (ESM 2c), which also suggests that labradorite dissolution in the plagioclase sample remained at an early stage. These observations suggest that the labradorite traces in the ilmenite sample react mostly in response to sulfide oxidation, whereas the trace sulfides in the plagioclase sample had practically no effect on labradorite dissolution. Thus, the labradorite dissolution in the pure plagioclase sample may be mainly due to CO_2-bearing deionized water leaching, which is much less aggressive than the leachates produced by sulfide oxidation in the pure ilmenite samples.

The evolution of the cumulative normalized values of elements related to sulfide oxidation, S, Ni, and Co, are presented in ESM 3a, 3b, and 3c respectively. The S release from ilmenite stabilized at a significantly higher rate than in the plagioclase sample (ESM 3a). The Ni and Co release from the plagioclase sample was insignificant, whereas Ni and Co release from the ilmenite progressively increased from approximately 100 days until approximately 450–475 days, after which Ni and Co releases appeared to slow down. The S release of the ilmenite sample also seemed to slow down at approximately 450–475 days. These release patterns suggest that Ni and Co was retained in the solids (most probably via sorption processes) during the first days, and that their release increased following the gradual saturation of the sorption sites. Finally, the decrease of Ni and Co release rates after 450–475 days, associated with a decrease in S release rates at the same time, is consistent with the previously stated hypothesis that sulfide oxidation is slowing down as a result of surface passivation and/or sulfide depletion, as described in many other studies (e.g. Benzaazoua et al. 2004; Cruz et al. 2001; Demers et al. 2008; Villeneuve et al. 2004).

ESM 5a compares the cumulative normalized loadings of Ca (y-axis) and Si (x-axis) in the pure minerals samples, while ESM 4a shows the same comparisons for waste rock samples. The cumulative Ca vs. Si loadings of the ilmenite sample stabilized at a lower slope (0.338; see Table 4) than the plagioclase sample (1.46; Table 4). This is most likely due to the fact that residual plagioclase in the ilmenite sample was leached more aggressively than in pure plagioclase, as discussed beforehand, and that its incongruent Ca dissolution progressed to a later stage (less Ca and more Si leached from the plagioclase; Plante et al. 2010a). The Ca, Si, and Al cumulative loadings (ESM 2a, 2b, and 2c respectively), and the comparison between the cumulative Ca and Si loadings (ESM 5a), are in accordance with the previously mentioned plagioclase reactivity sequence. In waste rocks samples, this reactivity sequence also explains the differences in Ca over Si releases (ESM 4a); the cumulative normalized Ca over Si slopes of the fresh waste rock samples (0.55–1.3; Table 4) are closer to those of the pure minerals (0.34–1.5) than the weathered waste rock samples (0.022–0.027).

The Mg and Mn generated by the pure minerals samples stabilized after 100 days (ESM 2d and 2e); the hemo-ilmenite sample generated more Mg and Mn than plagioclase, although the release rates stabilized at similar values (Table 4). The ilmenite sample contained approximately 1.6% Mg, 0.1% Mn (Table 2) as impurities in the ilmenite crystal lattice. Mg and Mn release during ilmenite dissolution is well known, and was described earlier in this paper. The cumulative loadings of Mg and Mn from the pure samples (ESM 5b) stabilized at slopes slightly lower (11–19; Table 4) than in fresh waste rocks (12–60; Table 4 and ESM 4b), while they stabilized at significantly higher slopes in weathered samples (64–129; Table 4 and ESM 4b). These results support the hypothesis that Mg is generated from another mineral than ilmenite in the waste rock samples, most likely the pyroxenes, which dissolve even faster in weathered samples than in fresh ones (Plante et al. 2010a), explaining the different Mg over Mn ratios obtained in this study. The Mg and Mn relation in ilmenite (ESM 5b) is also in agreement with the hypothesis that these elements are generated by ilmenite dissolution. The Mg and Mn slope obtained for plagioclase (19; Table 4) is close to the one in the hemo-ilmenite sample, but the total values generated are significantly lower, suggesting that they are generated (at least in part) by the ilmenite traces in the plagioclase and possibly other trace minerals, such as pyroxene (Table 3). Plante et al. (2010b) provides detailed characterization of the trace minerals in the Tio waste rocks.

The cumulative S vs. Ni loadings in the pure minerals (ESM 5c) stabilized at a significantly higher slope in the plagioclase sample (137; Table 4) than in the ilmenite sample (2.9; Table 4). This was due to the negligible cumulative Ni loadings in the plagioclase sample (ESM 3b); most Ni concentrations were below the method detection limit. In the waste rock samples, 4 of the 6 studied samples leached enough cumulative Ni loadings to generate release rates with $R^2 > 0.95$ (all samples except for C1 and C2; ESM 1f and Table 4) for the period considered in the linear regressions (after 200 days). For these samples, the cumulative S vs. Ni loadings stabilized at similar slopes (between 32 and 49; Table 4). While the S release rates of the waste rock samples were similar (ESM 1e and Table 4), it can be seen on ESM 1f that cumulative Ni loading of the C1 and C2 samples increased after 400 days. Comparison of the cumulative S and Ni loadings (ESM 4c) shows that they ultimately reached slopes similar to the other waste rock samples. It can also be observed in ESM 1f that the Ni release from the fresh samples began between 200 and 400 days, significantly later than the weathered waste rocks. This longer delay for the fresh samples to generate similar S and Ni release rates than the other samples is most likely due to Ni retention within the samples. It was previously demonstrated (Plante et al. 2010b) that the fresh waste rock samples were better able to retain Ni than the weathered ones, probably because the retention sites of the weathered samples were partly saturated during field weathering for approximately 25 years.

The Ni and Mn release also seem to be associated, both in the waste rocks (ESM 4d) and pure minerals (ESM 5d); the slopes of the cumulative Ni/Mn ratios are shown in Table 4. The Ni/Mn slopes are within one order of magnitude for waste rock samples (0.46–2.9), approximately one order of magnitude higher in the hemo-ilmenite sample (12), and approximately one order of magnitude lower (0.10) in the plagioclase sample. The Ni/Mn slopes of the weathered waste rocks were similar (2.4–2.9) and slightly higher than in fresh ones (0.46–2.0). The post-sorption Ni/Mn ratios (0.8–1.2) were within the range of those of the fresh waste rocks. The exact link between Ni and Mn release is not yet understood, but since Mn oxides are known to be effective Ni sorbents (e.g. Trivedi et al. 2001), Ni release may be linked to the solubility of Mn oxides within the waste rocks.

The results from the weathering cells on ilmenite and plagioclase samples illustrate that Ni was generated from the sulfides and not from the trace Ni levels within the ilmenite and plagioclase minerals, and that the ilmenite minerals possess a significant but limited Ni sorption capacity. They also illustrate that the Ca release from plagioclase in waste rock samples was a consequence of acid neutralization after sulfide oxidation rather than natural leaching.

Secondary Minerals

Secondary minerals are relatively rare in the fresh waste rocks, but are ubiquitous in weathered ones, as noticed over many SEM observations on the samples studied, both on polished sections and free grains (Plante 2010). Secondary minerals are also found more frequently in post-testing weathering cell samples of waste rocks and purified fractions than in initial waste rock samples. For example, a partially altered plagioclase particle (from the post-testing weathering cell plagioclase sample) seen under SEM (secondary electrons mode) is shown in Fig. 5, the left side being still relatively fresh while the right side shows alteration signs. EDS analyses (performed at the tip of the arrows) confirm the nature of the calcic plagioclase on the fresh portion of the particle, and suggest the presence of amorphous secondary minerals on the Ca- and Na-depleted altered plagioclase surface. This secondary phase contains Mg (coming from ilmenite and/or pyroxenes) and K (most probably released from mica minerals biotite and/or muscovite, see Table 3) that suggest illite precipitation ($(K,H_3O)(Al,Mg,Fe)_2(Si,Al)_4O_{10}[(OH)_2,(H_2O)]$; see Plante 2010); kaolinite may also be present in the amorphous alteration products on the plagioclase surfaces.

Ilmenite in the studied samples bears evidence of weathering: the fresh samples contained significantly less weathered ilmenite particles than weathered ones (C4–C6 and post-testing weathering cell C1–C3 samples). Many hemo-ilmenite particles observed under SEM (secondary electrons mode) also had secondary minerals at the surface (Fig. 6a) and in cracks (Fig. 6b), and EDS analyses (at arrow tips) suggest that these minerals contain Si, Al, and Mg (the strong Fe and Ti signals are generated from the adjacent ilmenite particles). Illite and kaolinite precipitation (secondary minerals) upon plagioclase weathering were demonstrated in another study on Tio waste rocks (Plante 2010; Plante et al. 2010a). Figure 6 shows an example of hemo-ilmenite particles (from the C6 sample) on polished sections (backscattered electrons mode) bearing evidence of heavy weathering, which leads to the formation of pseudorutile-like phases (ideally $Fe_2Ti_3O_9$) such as those described earlier. In the present study, a small portion of the observed pseudorutile phases had a trellis-like structure (Fig. 7a,c), suggesting leucoxene, described by Weibel (2003) as an alteration product of titanomagnetite (hematite in the present study) rather than ilmenite. However, the trellis structure observed in the present study seems to occur beside the hematite lamella (into the ilmenite) and not into the hematite lamella. Also, the hematite lamellas seem to be preserved in the process. The altered ilmenite grains shown on Fig. 7 all suggest that alteration proceeds from the surface inward and along fractures and weaknesses through the grains, as also observed by Lener (1997). Since the pseudorutile transformation into leucoxene involves incongruent dissolution (rather than Fe leaching as in the ilmenite-pseudorutile transformation), the trellis-like shape suggest leucoxenisation of the pseudorutile.

Metal Sorption Evaluation Through Sorption Cells

Fresh waste rock samples (C1–C3) in the sorption cells were leached with contaminated water for the first 325 days, after which they were leached with deionised

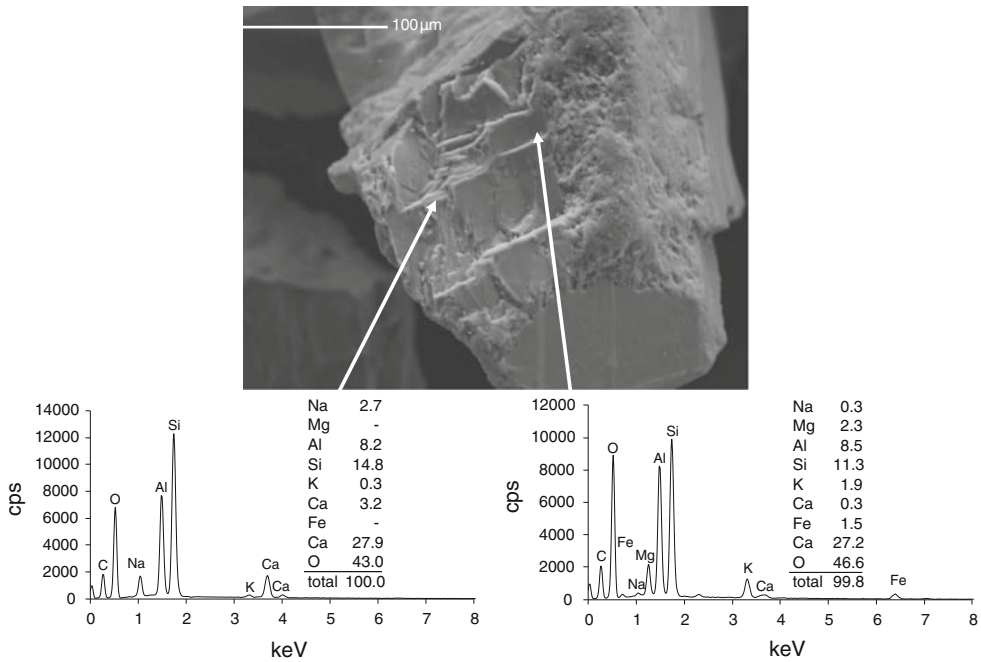

Fig. 5 SEM (secondary electrons mode) image of a plagioclase particle and EDS spectra of spot analyses on fresh (left) and altered (right) portion

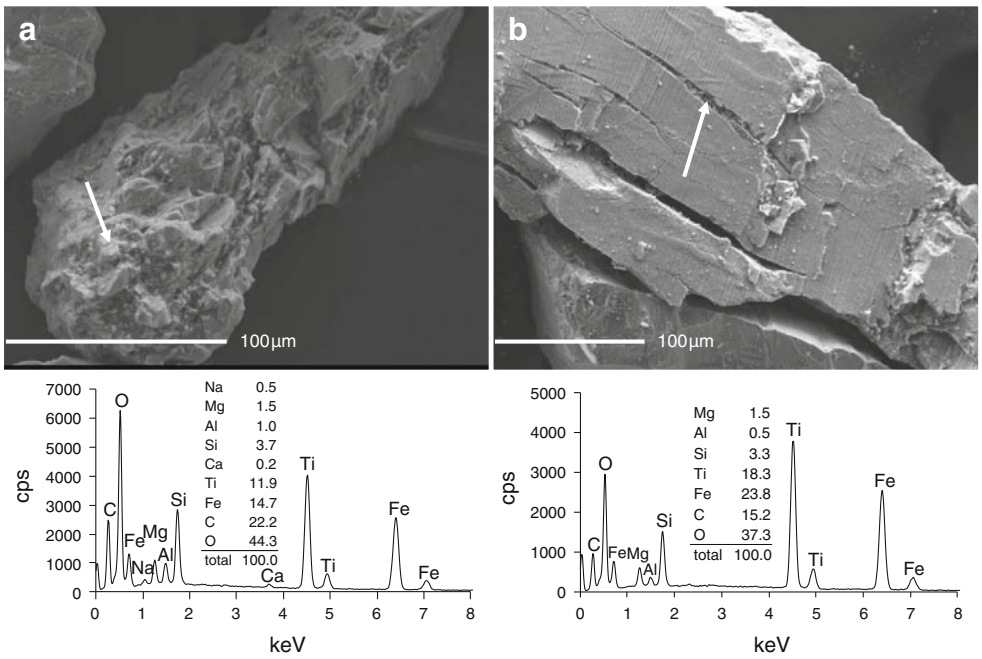

Fig. 6 SEM images (secondary electrons mode) showing weathered ilmenite particles; the corresponding EDS analyses are shown beneath each particle

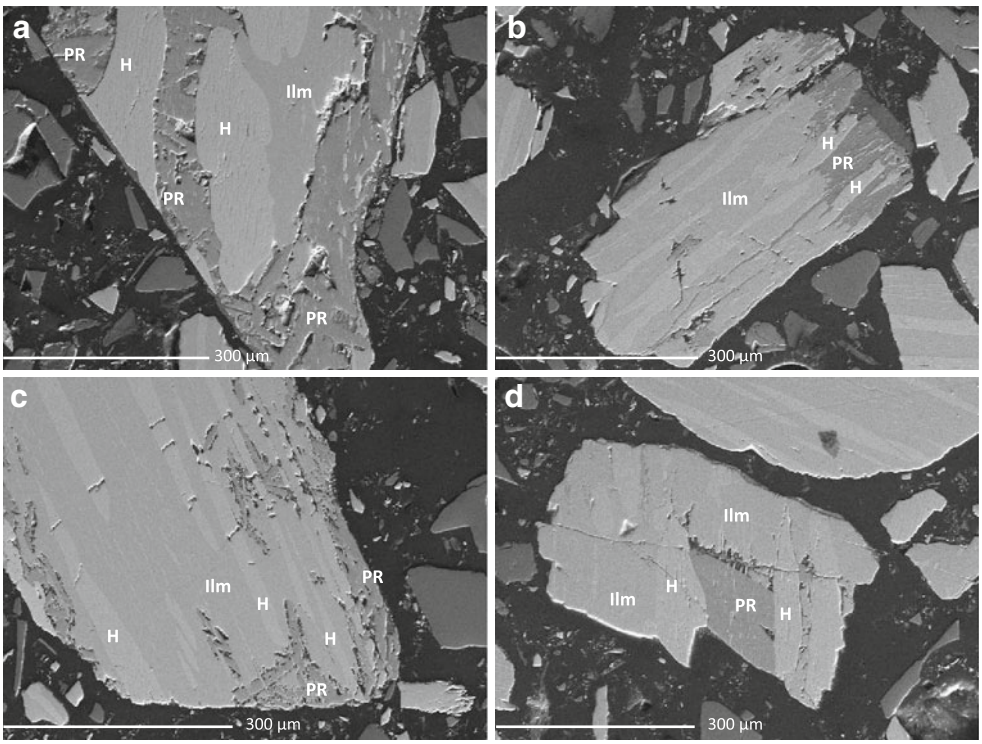

Fig. 7 SEM images (backscattered electrons mode) of weathered ilmenite from the C6 sample (H: hematite; Ilm: ilmenite; PR: pseudorutile-like phase)

water. Only the fresh waste rock samples were submitted to sorption cells, as it was believed (at the start-up of the sorption cells) that the weathered waste rocks capacities were saturated. The deionized water leaching enabled the evaluation of the stability of the previously sorbed phases under weathering cells conditions. The sorption cell results most relevant for the present study are shown in Fig. 8. The vertical dashed lines in Fig. 8 illustrate the transition

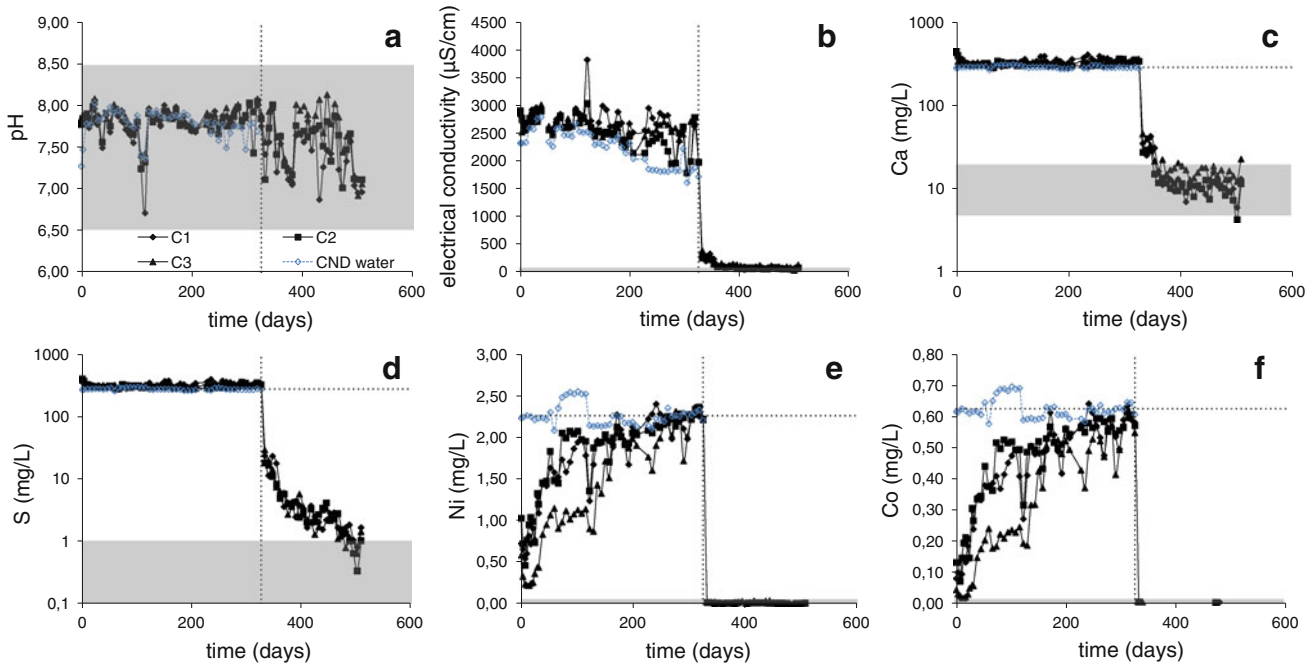

Fig. 8 Sorption cell results on fresh waste rock samples (note log scale for S); *shaded areas* represent fresh waste rock weathering cell ranges

between contaminated and deionized water leaching, whereas the horizontal dashed lines show the ion concentration in the contaminated water. The three fresh samples submitted to weathering cells show similar pH and conductivity results (Fig. 8a, b); the conductivity values significantly decreased during deionized water leaching (from >2000 to <150 µS/cm). Fig. 8c shows that Ca was generated in the sorption cells (the Ca levels are higher than the leaching water) but Ca concentrations significantly decreased to levels close to those of the weathering cells of fresh waste rocks upon deionized water leaching (around 10 mg/L; Fig. 2c). The Ni and Co concentrations in the leachates (shown in Fig. 8e f respectively) suggest that the sorption sites are gradually saturated (saturation reached at approximately 250 days) during the contaminated water leaching for this particular set of conditions, leading to metal levels in the leachates approximately equal to those of the contaminated water. These results also suggest that the sorbed Ni was stable under the conditions prevailing in weathering cells, as Ni and Co concentrations in the leachates produced with deionised water were very low. In fact, the Ni concentrations were in the same range as those obtained in the weathering cells of the fresh materials (Fig. 3b). The rapid decrease in metal concentrations within the first deionized water leachings suggest that the lag time before stabilization was caused by the remaining pore water containing CND water. Once the pore water was completely flushed out by the deionized water, the concentrations stabilized in the leachates.

The release rates of the sorption cells shown in Table 4 (C1-GR, C2-GR, and C3-GR post-sorption) were determined when the ion concentrations in the deionised water leaching stabilized, which occurred after approximately 400 days. The Ni release rates in sorption cells (2.0-3.4 E-3 mg/kg/d) were close to those in the weathering cells of the fresh samples (1.6 E-3 to 2.7 E -4 mg/kg/d). Thus, Ni and Co generated by sulfide oxidation could be sorbed in the weathering cells of the fresh waste rock samples, and the sorbed phases were stable under the prevailing conditions. The S release rates in the sorption cells when the ion levels in the deionised water leaching phase stabilized were about an order of magnitude higher (0.47–0.74 mg/kg/d) than in the weathering cells (0.04–0.06 mg/kg/d). This may be due to the dissolution of efflorescent sulfate salts that accumulated during the contaminated water leaching-drying cycles, as the contaminated water contained around 260 mg/L of S (approximately 780 mg/L as sulfate; see Fig. 8d). However, the S concentrations had not stabilized at the end of the sorption cell tests and were declining towards the range of concentrations in the weathering cells; consequently, the S release rates may have stabilized closer to those of the weathering cells if the test had been conducted for a longer period. The Ca release rates in sorption cells (2.8–3.1 mg/kg/d) were slightly higher than in weathering cells (1.4–2.4 mg/kg/d), again most probably because of the dissolution of the efflorescent salts. The same interpretation is valid for the comparison of the Mg release rates from the sorption and weathering cells. The Si

release rates from the sorption cells (0.5–0.8 mg/kg/d) are lower than from the weathering cells (1.8–2.5 mg/kg/d), though the generally low R^2 values obtained on those rates make these comparisons hazardous. However, the lower Si release rates in the sorption cells may be attributable to the formation of secondary Si-bearing minerals, a phenomenon that should be more intense in the sorption cell leachates because of their higher ion concentrations in the pore water.

The quantity of metal retained (q, in mg/g) in each sorption cell leaching was calculated, using Eq. 9, as the difference in metal concentration from the leaching water and the leached water: [9].

$$qi = \frac{(cf - c_{ini})v}{m} \quad (9)$$

The quantity of metal retained (q_i, in mg of metal per sample mass, or mg/g) in the leaching "i" was determined as the difference between the initial (C_{ini}) and final (C_f) metal concentrations (mg/L), times the leaching volume (L) divided by the sample mass (g). The profiles of the cumulative q_i values for Ni, Co, and Mn are shown in Fig. 9a, b, and c respectively. The cumulative Ni and Co retention profiles are similar for the waste rock samples; they increased rapidly with the first leachings and gradually slowed down as sorption sites were saturated. The sorption capacities peaked around 26–34 mg/kg for Ni and around 10–12 mg/kg for Co. Plante et al. (2010b) demonstrated that sorption phenomena were responsible for Ni retention in the Tio mine waste rocks. It can be hypothesised that the same is true for Co, since Ni and Co geochemical behaviour are similar. The $S_{sulfide}$ content in the waste rock samples follows C3 > C1 > C2, while the Ni content follows C2 ≈ C3 > C1, and the Co content follows C3 > C2 > C1 (Table 2). It is thus difficult to directly link the $S_{sulfide}$, Ni, and Co contents to the total sorption capacities, but these may have an impact in the total capacities, as evaluated by the sorption cell tests protocol employed.

The Mn retention profile is characterized by a gradual increase, followed by a peak (around 150 days) and finally by a decrease (meaning Mn is released in the leachates). The Mn retention capacities peaked at 2.0 mg/g for C1 and C2, and at 3.0 mg/g for the C3 waste rock sample. These peak Mn retention capacities decreased over 50% for the C1 waste rock sample (from 2.0 to less than 1.0 mg/g), while the decrease was on the order of 20% for C2 (from 2.0 to 1.6 mg/g), and 7% (from 3.0 to 2.8 mg/g) for C3. However, it remains unclear whether the Mn was retained in the weathering cells as a result of sorption, secondary minerals precipitation, or a combination of both. Surface studies, such as XPS, of Mn retention may provide more insight by revealing the Mn species involved.

The retention peaks obtained in the conditions of the sorption cells cannot be directly extrapolated to other conditions under which the Tio waste rocks were studied, such as weathering cells, humidity cells, and field tests. In fact, these retention peaks are only valid for the conditions under which they were obtained, under leaching from CND waters containing 2.26 mg/L Ni and 0.63 mg/L Co. Changing the composition of the leaching water will affect the retention profiles, but such effects were not measured in the present study. However, the results from the present study clearly indicated that the sorption capacities in a kinetic test (such as sorption and weathering cells) are limited, and that the sorbed species are stable.

The metal release rates from the sorption cells after stabilization in deionized water leachings are presented in Table 4 (C1, C2, and C3-GR post-sorption rates). The Ca, Mg, Mn, Ni, and S release rates in the sorption cells were all slightly higher (up to one order of magnitude) than those of the waste rock samples. The higher post-sorption release rates appear related to the saturation of the sorption sites. It is possible that the saturation of the retention sites during CND leaching leads to the higher release rates. However, further tests are needed to confirm this interpretation. Efflorescent salts of Ca, Mg, Mn, Ni, and S may have precipitated in the sorption cells as a consequence of the frequent leaching/drying cycles with CND water. The dissolution of such efflorescent salts with the post-sorption deionized water leachings could partly explain the higher

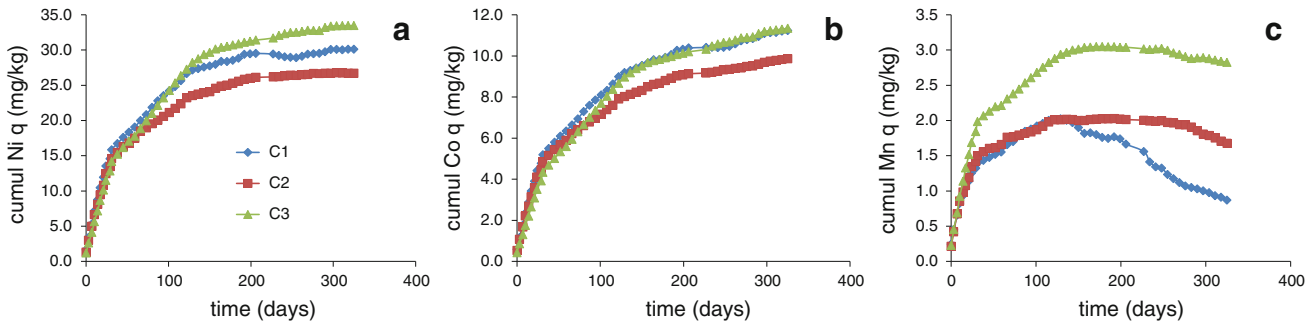

Fig. 9 Sorbed metal quantities (q) in sorption cells

Ca, Mg, Mn, Ni, and S release rates. However, the Si release rate is slightly lower in the sorption cells (post-sorption) than from the waste rock samples, in contradiction with the efflorescent salt hypothesis. Moreover, the post-sorption concentrations quickly drop to concentrations close to those of the corresponding weathering cells, suggesting that such efflorescent salts, if present, probably dissolved in the first post-sorption leaching cycles. Thus, the higher release rates of Ca, Mg, Mn, Ni, and S obtained post-sorption is likely associated with saturation of their sorption sites.

Conclusions and Recommendations

The main conclusions arising from the present study are:

The Ca release from plagioclase in waste rock samples is mainly a consequence of acid neutralization after sulfide oxidation and not natural leaching;

Ilmenite weathering releases Mg and Mn in drainage waters of the Tio mine waste rocks, but other gangue minerals also contribute to Mg and Mn release, particularly for Mg in weathered waste rocks, most probably by pyroxenes. Weathered ilmenite transforms into secondary pseudorutile and/or leucoxene phases in the Tio mine waste rocks;

Hematite doesn't seem to be dissolved in the Tio waste rocks in weathering cell conditions and in the field, but is probably implicated in metal sorption;

Secondary silicate minerals are ubiquitous in the Tio mine waste rocks and may play a significant role in Mg, Al, and Si (and possibly K) mobility in drainage waters;

Sorption phenomena are significant in fresh Tio mine waste rocks in weathering cells, and the sorbed Ni and Co phases are stable (when leached with deionized water) under the same conditions;

Sorbed or precipitated Mn phases seem to be unstable in weathering cell conditions;

The higher release rates of Ca, Mg, Mn, Ni, and S during deionized water leaching in sorption cells than in weathering cells may be explained by the saturation of sorption sites, although sorption phenomena involving Ca, Mg, Mn, and S needs to be investigated further to validate this hypothesis.

Results from the present study enabled a more precise evaluation of the CND generation potential from the Tio waste rocks. Even though the Ni concentrations obtained from the laboratory tests remain significantly lower than those obtained in field conditions (from field test pads and from waste rock piles), the results from the present study give important insight into the geochemical processes involved in CND generation.

However, some questions remain. More surface studies are needed to better understand Mn geochemistry in the Tio mine waste rocks as well as its role in Ni uptake. It is not clear how to scale up the weathering cells results to the field scale, and more precisely, why the Ni levels in the weathering cell leachates remain significantly lower than the Ni concentrations observed in the field. Finally, the behavior of weathered waste rocks is yet to be tested in sorption cell conditions.

Acknowledgments The authors thank the NSERC Polytechnique-UQAT Chair in Environment and Mine Wastes Management and the NSERC Collaborative Research and Development Grants for funding of this project. The authors also thank Donald Laflamme of Rio Tinto, Iron and Titanium, Inc., for the funding and constant support of this project, as well as Genevieve Pepin for providing samples and insight in the project. Alain Perreault, Mélanie Bélanger, and Mathieu Villeneuve of URSTM, UQAT are also acknowledged for their laboratory support during this project.

References

Benzaazoua M, Bussière B, Dagenais AM, Archambault M (2004) Kinetic tests comparison and interpretation for prediction of the Joutel tailings acid generation potential. Environ Geol 46:1086–1101

Blake RE, Walter LM (1999) Kinetics of feldspar and quartz dissolution at 70–80°C and near-neutral pH: effects of organic acids and NaCl. Geochim Cosmochim Acta 63:2043–2059

Blum AE, Stillings LL (1995) Feldspar dissolution kinetics. Rev Mineral Geochem 31:291–351

Brunauer S, Emmett PH, Teller E (1938) Adsorption of gases in multimolecular layers. J Am Chem Soc 60:309–319

Bussière B (2007) Colloquium 2004: Hydrogeotechnical properties of hard rock tailings from metal mines and emerging geoenvironmental disposal approaches. Can Geotech J 44:1019–1052

Carroll SA, Knauss KG (2005) Dependence of labradorite dissolution kinetics on CO2(aq), Al(aq), and temperature. Chem Geol 217:213–225

Casey WH, Westrich HR, Massis T, Banfield JF, Arnold GW (1989) The surface of labradorite feldspar after acid hydrolysis. Chem Geol 78:205–218

Cruz R, Mendez BA, Monroy M, Gonzalez I (2001) Cyclic voltammetry applied to evaluate reactivity in sulfide mining residues. Appl Geochem 16:1631–1640

Demers I, Bussière B, Benzaazoua M, Mbonimpa M, Blier A (2008) Column test investigation on the performance of monolayer covers made of desulphurized tailings to prevent acid mine drainage. Miner Eng 21:317–329

Frost MT, Grey IE, Harrowfield IR, Mason K (1983) The dependence of alumina and silica contents on the extent of alteration of weathered ilmenites from Western Australia. Mineral Mag 47: 201–208

Grey IE, Reid AF (1975) The structure of pseudorutile and its role in the natural alteration of pseudorutile. Am Mineral 60:898–906

Grey I, MacRae C, Silvester E, Susini J (2005) Behaviour of impurity elements during the weathering of ilmenite. Mineral Mag 69: 437–446

Hellmann R (1995) The albite-water system: part ii. The time-evolution of the stoichiometry of dissolution as a function of pH at 100, 200, and 300°C. Geochim Cosmochim Acta 59(9):1669–1697

Hodgkinson J, Cox ME, McLoughlin S (2008) Coupling mineral analysis with conceptual groundwater flow modelling: the source

and fate of iron, aluminium and manganese in a back-barrier island. Chem Geol 251:77–98
Inskeep WP, Nater EA, Bloom PR, Vandervoort DS, Erich MS (1991) Characterization of laboratory weathered labradorite surfaces using x-ray photoelectron spectroscopy and transmission electron microscopy. Geochim Cosmochim Acta 55:787–800
Janßen A, Golla-Schindler U, Putnis A (2008) The mechanism of ilmenite leaching during experimental alteration in HCl-solution. In: Proceedings of EMC 14th European Microscopy Congress, Aachen, Germany. pp 825–826
Klein C, Hurlbut CS Jr, after Dana JD (1977) Manual of Mineralogy, 20th edit, John Wiley and Son, New York City. NY, USA, p 596
Lawrence RW, Wang Y (1997) Determination of neutralization potential in the prediction of acid rock drainage. Proc, 4th International Conf on Acid Rock Drainage (ICARD). Vancouver, Canada, pp 451–464
Lener EF (1997) Mineral chemistry of heavy minerals in the Old Hickory Deposit, Sussex and Dinwiddie Counties, Virginia. PhD Thesis, Virginia Polytechnic Institute and State University, Blacksburg, VA, USA
MEND (2004) Review of Water Quality Issues in Neutral pH Drainage: Examples and Emerging Priorities for the Mining Industry in Canada. Report 10.1, Ottawa, Canada
Merkus HG (2009) Particle size measurements: fundamentals, practice, quality. Particle Technology Series, vol 17, Springer Science Business Media BV, ISBN: 978-1-4020-9015-8 (Print), 978-1-4020-9016-5 (Online). doi:10.1007/978-1-4020-9016-5_6, 536 pp
Mücke A, Bhadra Chaudhuri JN (1991) The continuous alteration of ilmenite through pseudorutile to leucoxene. Ore Geol Rev 6:25–44
Muir IJ, Nesbitt HW (1992) Controls on differential leaching of calcium and aluminum from labradorite in dilute electrolyte solutions. Geochim Cosmochim Acta 56(11):3979–3985
Muir IJ, Nesbitt HW (1997) Reactions of aqueous anions and cations at the labradorite-water interface: coupled effects of surface processes and diffusion. Geochim Cosmochim Acta 61:265–274
Muir IJ, Bancroft MG, Nesbitt WH (1989) Characteristics of altered labradorite surfaces by SIMS and XPS. Geochim Cosmochim Acta 53:1235–1241
Muir IJ, Bancroft MG, Shotyk W, Nesbitt WH (1990a) A SIMS and XPS study of dissolving plagioclase. Geochim Cosmochim Acta 54:2247–2256
Muir IJ, Bancroft GM, Nesbitt HW (1990b) Analysis of dissolved plagioclase mineral surfaces. Surf Interface Anal 16:581–582
Nair AG, Suresh Babu DS, Damodaran KT, Shankar R, Prabhu CN (2009) Weathering of ilmenite from Chavara deposit and its comparison with Manavalakurichi placer ilmenite, southwestern India. J Asian Earth Sci 34:115–122
Nesbitt HW, Skinner WM (2001) Early development of Al, Ca, and Na compositional gradients in labradorite leached in pH 2 HCl solutions. Geochim et Cosmochim Acta 65(5):715–727
Nicholson RV (2004) Overview of near neutral pH drainage and its mitigation: results of a MEND study. MEND Ontario workshop, Sudbury, Canada
Oelkers EH, Schott J (2001) An experimental study of enstatite dissolution rates as a function of pH, temperature, and aqueous Mg and Si concentration, and the mechanism of pyroxene/pyroxenoid dissolution. Geochim Cosmochim Acta 65:1219–1231
Oelkers EH, Golubev SV, Chairat C, Pokrovsky OS, Schott J (2009) The surface chemistry of multi-oxide silicates. Geochim Cosmochim Acta 73:4617–4634
Pepin G (2009) Évaluation du comportement géochimique de stériles potentiellement générateurs de drainage neutre contaminé à l'aide de cellules expérimentales in situ. MS degree, Dépt des génies civil, géologique et des mines. École Polytechnique de Montréal, Montreal, Québec, Canada
Pepin G, Bussière B, Aubertin M, Benzaazoua M, Plante B, Laflamme D, Zagury GJ (2008) Field experimental cells to evaluate the generation of contaminated neutral drainage by waste rocks at the Tio mine, Quebec, Canada. Proc, 10th International Mine Water Assoc (IMWA) Congress on Mine Water and the Environment, Czech Republic, pp 309–312
Pettit CM, Scharer JM, Chambers DB, Halbert BE, Kirkaldy JL, Bolduc L (1999) Neutral mine drainage. Proc, Sudbury 1999 Mining and the Environment International Conference. vol 2, pp 829–838
Plante B (2005) Comparaison des essais statiques et évaluation de l'effet de l'altération pour des rejets de concentrateur à faible potentiel de génération d'acide. Dépt des génies civil, géologique et des mines. École Polytechnique de Montréal. Montréal, Québec, Canada
Plante B (2010) Prédiction du drainage neutre contaminé en Ni: cas de la mine Tio. Ph.D. thesis, Université du Québec en Abitibi-Témiscamingue (UQAT), Québec, Canada
Plante B, Benzaazoua M, Bussière B, Pepin G, Laflamme D (2008) Geochemical behaviour of nickel contained in Tio mine waste rocks. In: Rapantova, N., Hrkal, Z. (Eds) Proc, 10th International Mine Water Assoc (IMWA) Congress on Mine Water and the Environment, Czech Republic, pp 317–320
Plante B, Benzaazoua M, Bussière B (2010a) Predicting Geochemical Behaviour of Waste Rock with Low Acid Generating Potential Using Laboratory Kinetic Tests. Mine Water Environ (in press) doi:10.1007/s10230-010-0127-z
Plante B, Benzaazoua M, Bussière B, Biesinger MC, Pratt AR (2010b) Study of Ni sorption onto Tio mine waste rock surfaces. Appl Geochem (in press). doi:10.1016/j.apgeochem.2010.09.010
Price WA, Kwong YTJ (1997) Waste Rock Weathering, sampling and analysis: observations from the British Columbia Ministry of Employment and Investment database. Proceedings of 4th International Conf on Acid Rock Drainage (ICARD). Vancouver, Canada, pp 31–45
Rietveld HM (1993) The Rietveld Method. Oxford Univ Press, London, UK
Sapsford DJ, Bowell RJ, Dey M, Williams KP (2009) Humidity cell tests for the prediction of acid rock drainage. Min Eng 22:25–36
Schroeder PA, Le Golvan JJ, Roden MF (2002) Weathering of ilmenite from granite and chlorite schist in the Georgia Piedmont. Am Mineral 87:1616–1625
Schweda P, Sjöberg L, Södervall U (1997) Near-surface composition of acid-leached labradorite investigated by SIMS. Geochim Cosmochim Acta 61:1985–1994
Sobek AA, Schuller WA, Freeman JR, Smith RM (1978) Field and laboratory methods applicable to overburdens and minesoils. EPA-600/2–78-054. Washington, DC, USA, pp 47–50
Stefánsson A (2001) Dissolution of primary minerals of basalt in natural waters: I. calculation of mineral solubilities from 0°C to 350°C. Chem Geol 172:225–250
Trivedi P, Axe L, Tyson TA (2001) Xas studies of ni and zn sorbed to hydrous manganese oxide. Environ Sci Technol 35(22):4515–4521
Villeneuve M, Bussière B, Benzaazoua M, Aubertin M, Monroy M (2004) The influence of kinetic test type on the geochemical response of low acid generating potential tailings. Proc, Tailings and Mine Waste '03, Sweets and Zeitlinger. Vail, CO, USA, pp 269–279
Weibel R (2003) Alteration of detrital Fe-Ti oxides in Miocene fluvial deposits, central Jutland, Denmark. Bull Geol Soc Den 50:171–183
Zakaznova-Herzog VP, Nesbitt HW, Bancroft GM, Tse JS (2008) Characterization of leached layers on olivine and pyroxenes using high-resolution XPS and density functional calculations. Geochim Cosmochim Acta 72(1):69–86